

Comparative study of the synthesis of CoFe_2O_4 and NiFe_2O_4 in silica through the polymerized complex route of the sol–gel method

Sagrario M. Montemayor · L. A. García-Cerda ·
J. R. Torres-Lubián · O. S. Rodríguez-Fernández

Received: 27 September 2006 / Accepted: 9 January 2007 / Published online: 8 March 2007
© Springer Science + Business Media, LLC 2007

Abstract In this work the synthesis of $\text{CoFe}_2\text{O}_4\text{-SiO}_2$ and $\text{NiFe}_2\text{O}_4\text{-SiO}_2$ nanocomposites was studied via the sol–gel method, using the polymerized complex route. The polymerized precursors obtained by the reaction of citric acid, ethylene glycol, tetraethylorthosilicate, ferric nitrate, and cobalt nitrate or nickel chloride were characterized by nuclear magnetic resonance (NMR) and infrared (IR) spectroscopy. NMR and IR spectra of the precursors, without and with metallic ions, show the formation of polymeric chains with ester and ether groups and complexes of metal-polymeric precursor. The nanocomposites were obtained by the thermal decomposition of the organic fraction and characterized by X-ray diffraction (XRD) and vibrating sample magnetometry (VSM). XRD patterns show the formation of CoFe_2O_4 and NiFe_2O_4 in an amorphous silica matrix above 400°C in both cases. When the calcination temperature was 800°C the particle size of the crystalline phases, calculated using the Scherrer equation, reached ~ 35 nm for the two oxides. VSM plots show the ferrimagnetic behavior that is expected for this type of magnetic material; the magnetization at 12.5 KOe of the $\text{CoFe}_2\text{O}_4\text{-SiO}_2$ and $\text{NiFe}_2\text{O}_4\text{-SiO}_2$ compounds was 29.5 and 17.4 emu/g, respectively, for samples treated at 800°C .

Keywords CoFe_2O_4 · NiFe_2O_4 · Polymerized complex route · Sol–gel method

1 Introduction

In bulk form, cobalt and nickel ferrites are magnetic compounds useful in many technological applications [1]. But also, when these compounds are synthesized by techniques such as the polymerized complex method [2], continuous hydrothermal synthesis [3], or microemulsion [4], nanoscale particles are obtained, that can be employed in important applications, such as magnetocaloric refrigeration [5], ferrofluid technology [6], and magnetically guided drug delivery [7]. However, it is well known that magnetic nanoparticles tend to agglomerate, due to their large surface energies and strong magnetic interactions [8]. For this reason, some nanoscale magnetic materials are synthesized by dispersing the particles in inert matrixes, such as amorphous silica or polymers [9, 10]. On the other hand, the synthesis route of the polymerized complex of the sol–gel method has been used to obtain several mixed oxides [11], especially ferrites of nickel [12], nickel-zinc [13] and strontium [14]. This method presents a better control in the stoichiometry of the products, use lower synthesis temperatures and shorter reaction times with respect to other synthesis routes, especially the solid state reaction method, which is the route often used to obtain oxides [11]. In addition, the polymerized complex method give better reproducibility compared to the solid state reaction method.

Here we report a comparative study of the synthesis of two nanocomposites of $\text{CoFe}_2\text{O}_4\text{-SiO}_2$ and $\text{NiFe}_2\text{O}_4\text{-SiO}_2$, through the polymerized complex route of the sol–gel method and the NMR and IR characterization of the polymerized precursors.

S. M. Montemayor (✉) · L. A. García-Cerda ·
J. R. Torres-Lubián · O. S. Rodríguez-Fernández
Centro de Investigación en Química Aplicada, Boulevard Enrique
Reyna Hermosillo No. 140,
Saltillo, Coahuila, C. P. 25253, México
e-mail: smmontemayor@ciqa.mx or
smartinezmontemayor@yahoo.com.mx

2 Experimental

The starting chemicals used in this work were citric acid (CA), ethylene glycol (EG), iron nitrate ($\text{Fe}(\text{NO}_3)_3 \cdot 9\text{H}_2\text{O}$), cobalt nitrate ($\text{Co}(\text{NO}_3)_2 \cdot 6\text{H}_2\text{O}$), nickel chloride ($\text{NiCl}_2 \cdot 4\text{H}_2\text{O}$) tetraethylorthosilicate (TEOS) and ethanol of reagent grade (> 98%) purchased from Aldrich.

The appropriate amounts of CA (9 mol) and EG (22.5 mol) were mixed and stirred at room temperature in order to obtain a transparent solution. Cobalt or nickel (1 mol), respectively, and iron (2 mol) salts were added and the mixtures were stirred to achieve complete solubility. TEOS (3 mol) was then added, which was immiscible, followed by addition of ethanol to solubilize the TEOS. The solutions were heated at 130 °C for 2 h at 80 mm Hg in order to promote the polyesterification and completely remove the residual water and EG. During this reaction, the solution became more viscous and showed no turbidity. This viscous gel is called the “polymerized complex”. The polymerized complex was cross-linked by heating at 130 °C for 7 days in an oven. This resulted in a brown solid mass, which was grounded into a powder with a planetary mill. The powder was then heat treated at 400, 600, 800 and 1000 °C for 2 h in a furnace. For the purpose of comparison, a “polymeric precursor” without metal ions was prepared, following the same procedure, except for the thermal treatments.

2.1 Characterization of precursors

All 1D (^1H and ^{13}C) and 2D (HETCOR)-NMR spectra were collected at room temperature in D_2O , using a Jeol-Eclipse-300 spectrometer at frequencies of 300 and 75.4 MHz for ^1H and ^{13}C , respectively. IR spectra ($4000\text{--}500\text{ cm}^{-1}$) were recorded on KBr pellets using a Thermo-Nicolet/Nexus 470 spectrometer.

2.2 Characterization of nanocomposites

XRD spectra were obtained using a Siemens D5000 X-ray diffractometer ($\text{Cu K}\alpha$, $\lambda = 1.5418 \text{ \AA}$) in a 2θ range of 10 to 80° with a step size of 0.02°/s. Magnetic properties of the samples were measured with a Lake Shore 7300 vibrating sample magnetometer in applied fields from -12.5 to 12.5 KOe. Transmission micrographs were taken using a Jeol JEM 1200EXII microscope operated at 60 KV.

3 Results and discussion

3.1 Characterization of precursors

Figure 1 shows a two-dimensional NMR plot (HETCOR experiment) of the polymeric precursor without metal ions, where the ^{13}C and ^1H spectra are correlated. Both ^{13}C and ^1H spectra show resonances that correspond to carbon or proton centers, respectively, that arise from methyl and methylene groups of CA, EG and TEOS after the esterification, etherization and substitution reactions [15], according to chemical shift values (Table 1) and corroborated in this figure by the correlation between carbon and hydrogen signals remarked with dot lines. Letters are used to indicate the signals ascribed to the carbon (lower case) and hydrogen (upper case) centers in the scheme presented in the figure.

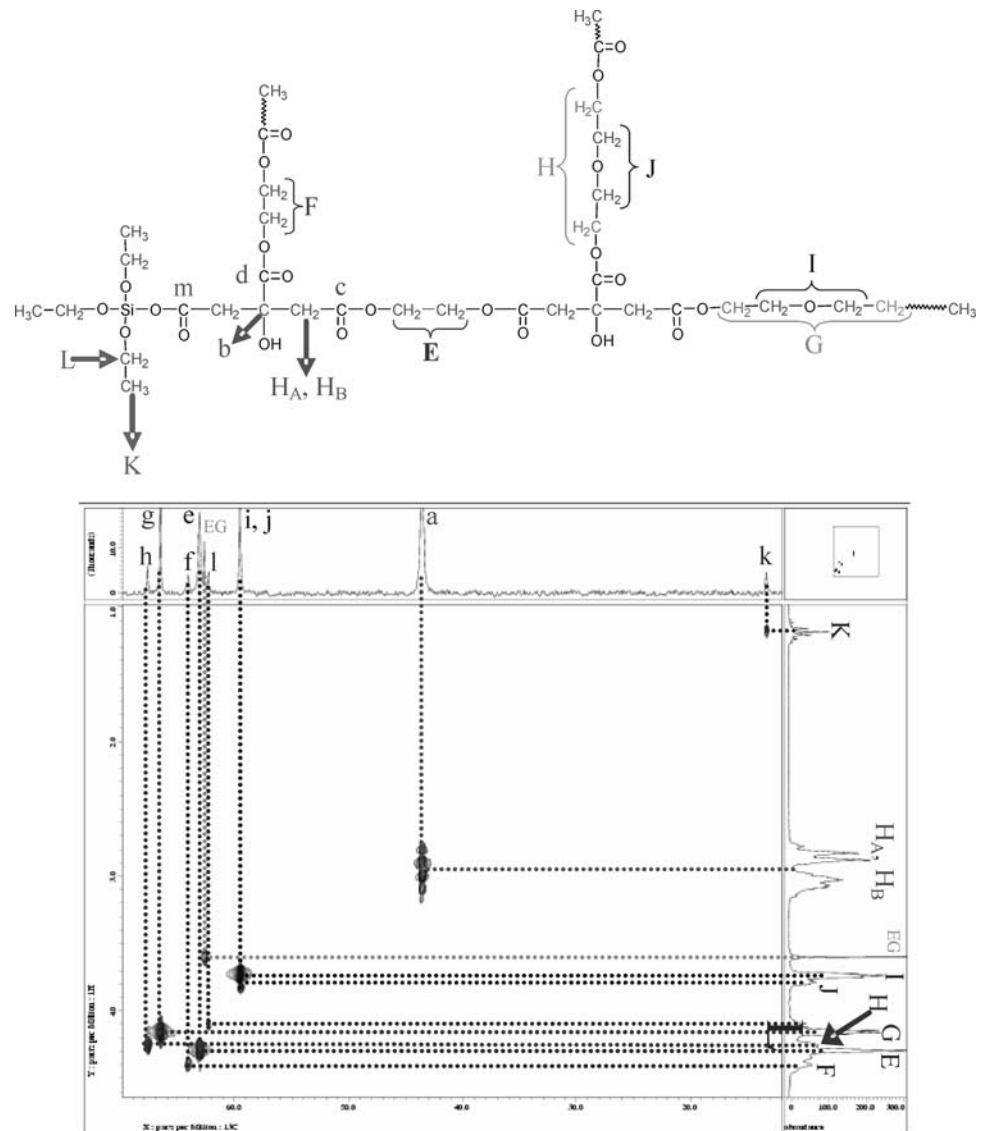
The polymerized complexes with iron and cobalt or iron and nickel show NMR spectra similar that of the polymeric precursor without metal ions, although they are broader (especially in the case of ^1H -NMR) and the base line is noisier due to the presence of the paramagnetic ions [16].

The formation of the polymerized complex in the two precursors synthesized with the metal ions, Fe(III)-Co(II) and

Table 1 ^{13}C and ^1H chemical shifts for different moieties

		Chemical shifts			
		^{13}C			^1H
$-\text{CH}_2-$	a	43.8	H_A , H_B		2.6, 2.8
C	b	73.8	–		–
O=C	c	171.3	–		–
O=C	d	173.5	–		–
$-\text{O}-\text{CH}_2-$	e	63.2	E		4.3
$-\text{O}-\text{CH}_2-$	f	64.2	F		4.32–4.48
$-\text{O}-\text{CH}_2-$	g	66.7	G		4.16
$-\text{O}-\text{CH}_2-$	h	67.8	H		4.26
$-\text{CH}_2-\text{O}-$	i	59.6	I		3.75
$-\text{CH}_2-\text{O}-$	j	59.6	J		3.82
$-\text{CH}_3$	k	13.4	K		1.2
$-\text{CH}_2-\text{O}-\text{Si}-$	l	62.2	L		4.1
O=C		174.5	–		–
	m	176.42	–		–

Fig. 1 HETCOR plot of the precursor without metal ions



Fe(III)-Ni(II), is demonstrated by the presence of two IR bands at ~ 1624 and $\sim 1400\text{ cm}^{-1}$, which are attributable to the carboxylate groups arising from the reaction of CA, EG and TEOS being coordinated to the metal ions [17]. The comparison between the IR spectra of polymeric precursor, polymerized complex with iron and cobalt and polymerized complex with iron and nickel, is shown in Fig. 2. All the spectra contain a broad band at $\sim 3400\text{ cm}^{-1}$ due to the O–H stretching modes of the hydroxyl groups in the precursors and to the intermolecular hydrogen bonds [17]. In addition, there are two bands related to C=O and C–O stretching vibrations of the ester groups [17] at ~ 1730 and $\sim 1185\text{ cm}^{-1}$, respectively, and another band at $\sim 1075\text{ cm}^{-1}$, which could be associated with Si–O stretching vibrations [18]. The polymerized complexes with Fe(III) [19], Y(III) and Fe(III) [17], Li(I) and Co(II) [20], reported previously, show analogous bands at the same frequencies.

3.2 Characterization of nanocomposites

The comparative study of the formation of the $\text{CoFe}_2\text{O}_4\text{-SiO}_2$ and $\text{NiFe}_2\text{O}_4\text{-SiO}_2$ nanocomposites as a function of sintering temperature by X-ray diffraction is showed in the Fig. 3. In both cases it is possible to observe an improvement in the crystallinity of magnetic phase as a function of the increase in temperature during thermal treatment. The spectra of the samples sintered above $400\text{ }^\circ\text{C}$ show a clear correspondence with reported patterns of CoFe_2O_4 and NiFe_2O_4 (JCPDS cards: 22-1086 and 10-0325, respectively). The samples sintered at $1000\text{ }^\circ\text{C}$ show a diffraction peak (identified as * in the figure) associated with the crystallization of amorphous SiO_2 to quartz (JCPDS 11-0252). The average size of crystallites in the samples of the two nanocomposites was calculated using Scherrer equation [21] and the most intense diffraction peaks. The growth of crystallites with increasing sintering

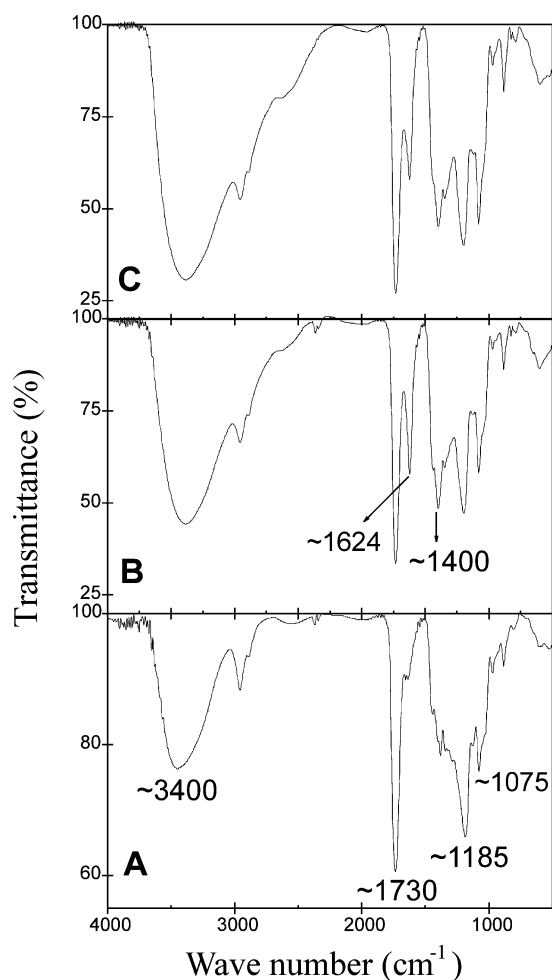


Fig. 2 IR spectra of precursor without metallic ions (A), polymerized complex with iron and cobalt (B) and polymerized complex with iron and nickel (C)

temperature is shown next to the strongest peak in the patterns of Fig. 3. In the samples with quartz (1000 °C), the ferrite particles do not grow so much as in the samples treated at 800 °C, where crystallization silica does not occur.

The hysteresis loops of the two nanocomposites heated at 800 °C (Fig. 4) show the ferrimagnetic behavior characteristic of CoFe_2O_4 and NiFe_2O_4 [8]. Since the composition and the average size of the particles affect the saturation magnetization values [22], these values differ, in our case, for: (1) samples with cobalt or nickel and (2) samples with thermal treatments at different temperatures. The magnetization values at 12.5 KOe increased with particle size (Table 2). This tendency has been observed in other magnetic materials [23]. The maximum magnetizations were reached in the nanocomposites at 800 °C; their values were 29.5 and 17.4 emu/g for $\text{CoFe}_2\text{O}_4\text{-SiO}_2$ and $\text{NiFe}_2\text{O}_4\text{-SiO}_2$, respectively. These values are approx 70% of the room temperature saturation values of Co and Ni ferrites (80 and 50 emu/g, respectively) at a 50% loading. Nanoscale magnetic particles

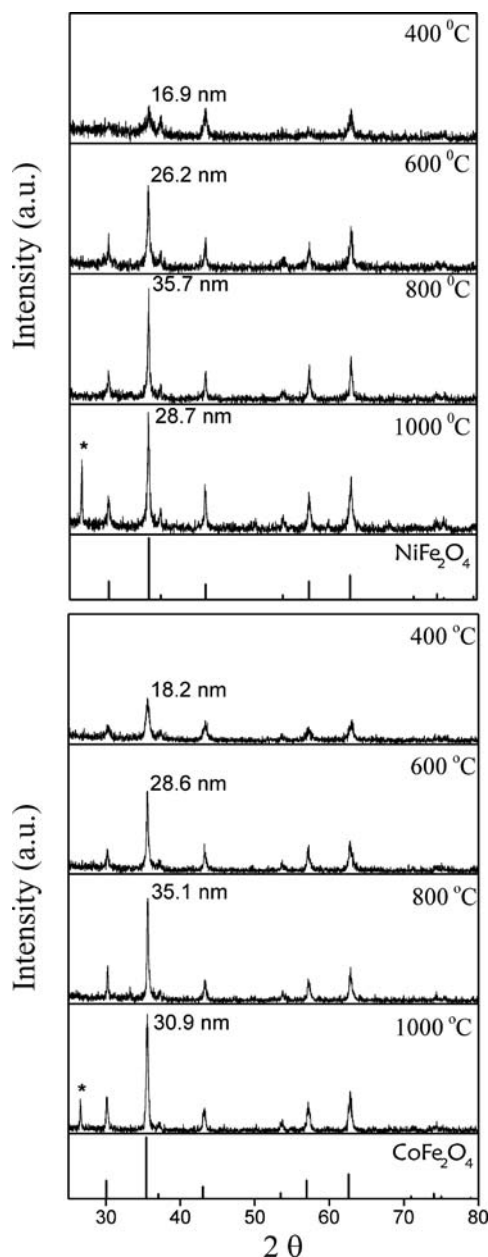


Fig. 3 Structural evolution of $\text{CoFe}_2\text{O}_4\text{-SiO}_2$ and $\text{NiFe}_2\text{O}_4\text{-SiO}_2$ as a function of temperature

typically show magnetization values lower than expected due to surface effects [24]. In addition, the magnetization values reported here are not saturation values.

Figure 5 shows the micrographs of the $\text{CoFe}_2\text{O}_4\text{-SiO}_2$ and $\text{NiFe}_2\text{O}_4\text{-SiO}_2$ nanocomposites obtained sintering the polymeric complexes at 800 °C. In these images it is possible to observe the nanoparticles, as dark spots in the photograph, homogeneously dispersed in the amorphous silica matrix. The size of the particles in both nanocomposites varies from 10 to 35 nm approximately.

The results obtained in this work are interesting by themselves and additionally, when compared to those presented

Table 2 Saturation magnetization values as a function of average particle size of nanocomposites

CoFe ₂ O ₄		NiFe ₂ O ₄	
Size (nm)	Ms (emu/g)	Size (nm)	Ms (emu/g)
18.2	13.2	16.9	7.9
28.6	20.1	26.2	11.2
30.9	25.3	28.7	14.7
35.1	29.5	35.7	17.4

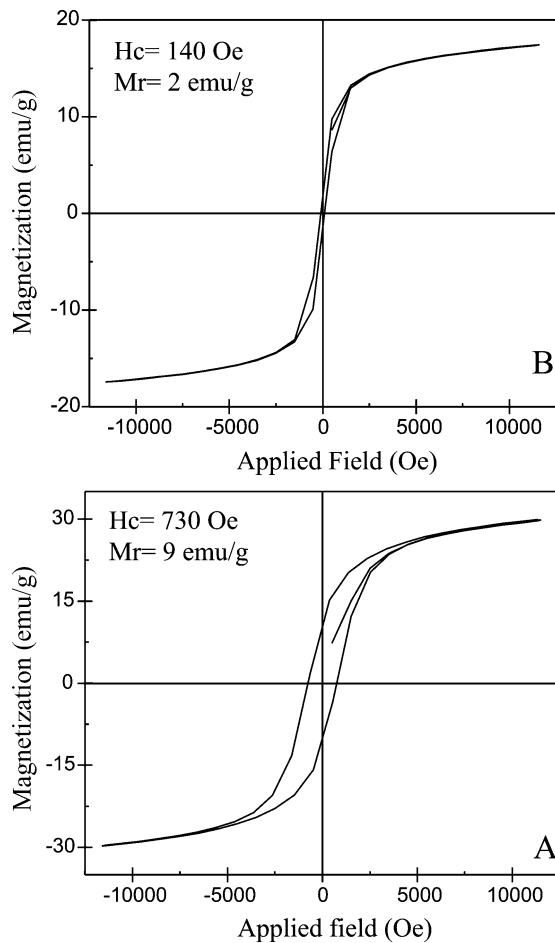


Fig. 4 Hysteresis loops of nanocomposites of CoFe₂O₄-SiO₂ (A) and NiFe₂O₄-SiO₂ (B), prepared at 800 °C

previously by some of us regarding the synthesis of CoFe₂O₄ nanoparticles by a similar approach to the one used in this paper [2]. In that case, CoFe₂O₄ nanoparticles (without the silica matrix) obtained at 800 °C had a ferrimagnetic behavior, a magnetization value of 79.8 emu/g at 12.5 KOe and an average particle size of 56 nm (XRD) and ~30–50 nm (TEM). The differences between the results obtained in both papers are a consequence of the presence of the silica matrix which constraint the CoFe₂O₄ nanoparticles growth.

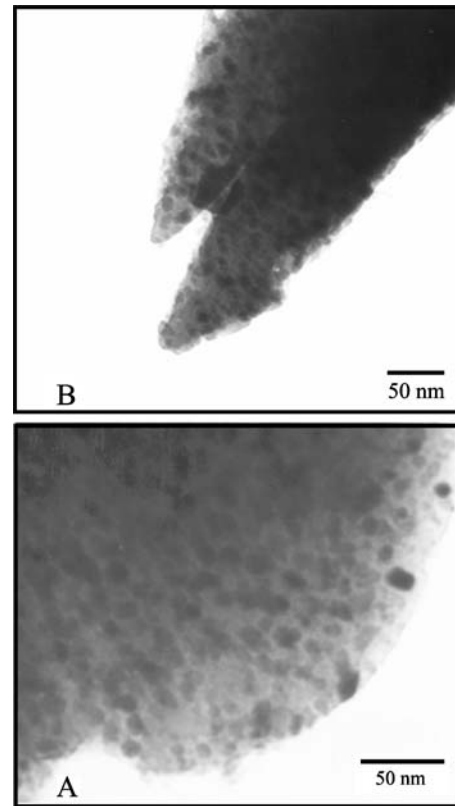


Fig. 5 TEM micrographs of the CoFe₂O₄-SiO₂ (A) and NiFe₂O₄-SiO₂ (B) nanocomposites sintered at 800 °C

4 Conclusions

The esterification, etherization and substitution reactions between CA, EG and TEOS lead to the polymeric precursor presented in this work. In addition, in the presence of metallic salts result in the formation of precursors bonded to the metal ions. As such, these precursors may be useful in the preparation of homogeneous dispersion for Co and Ni ferrites in amorphous silica at the low temperature of 800 °C.

Acknowledgments We thank CINVESTAV-IPN Unidad Saltillo for VSM measurements, María Antonieta Medina for editorial comments and especially we thank to PhD. Ronald F. Ziolo for reading and correcting the final version of this manuscript. Sagrario M. Montemayor thanks CONACyT-México for the scholarship 118728. This work was partially supported by CONACyT-México under project SEP-2004-CO1-46302.

References

- O’Handley RC (1999) Modern magnetic materials. Wiley Interscience, USA
- Montemayor SM, García-Cerda LA, Torres-Lubián JR (2005) Mater Lett 59:1056
- Cote LJ, Teja AS, Wilkinson AP, Zhang ZJ (2003) Fluid Phase Equilibria 210:307

4. Rondinone AJ, Samia ACS, Zhang ZJ (1999) *J Phys Chem B* 103:6876
5. McMichael RD, Shull RD, Swartzendruber LJ, Bennet LH (1992) *J Magnetism and Magnetic Mater* 111:29
6. Raj K, Moskowitz R, Casciari R (1995) *J Magnetism Magnetic Mater* 149:174
7. Häfeli U, Shütt W, Teller J, Zborowsky M (1997) *Scientific and clinical applications of magnetic carriers*. Plenum, NY
8. Valenzuela R (1994) *Magnetic ceramics*. Cambridge University Press, Cambridge
9. Wu KH, Huang WC (2004) *J Solid State Chem* 177:3052
10. Ahmed SR, Kofinas P (2002) *Macromolecules* 35:3338
11. Kakihana M (1996) *J Sol-Gel Sci Technol* 6:7
12. Prasad S, Gajbhiye NS (1998) *J Alloys Comp* 265:87
13. Verma A, Goel TC, Mendiratta RG, Kishan P (2000) *J Magnetism Magnetic Mater* 208:13
14. García-Cerda LA, Rodríguez-Fernández OS, Reséndiz-Hernández PJ (2004) *J Alloys Comp* 369:182
15. Pourchet CJ, Behnke J (1993) *The Aldrich library of ^{13}C and ^1H FT NMR spectra, vol 1 (1st edn.)* Aldrich Chemical Co, Milwaukee, WI
16. Friebolin H (1991) *Basic one and two dimensional NMR spectroscopy*. VCH Editorial, USA
17. Todorovsky DS, Dumanova DG, Todorovska RV, Getsova MM (2002) *Croatica Chemica Acta* 75:155
18. Huang X, Chen Z (2004) *J Crystal Growth* 271:287
19. Todorovska RV, Zotova StG, Todorovsky DS (2002) *Mater Lett* 56:770
20. Zhecheva E, Stoyanova R, Gorova M, Alcántara R, Morales J, Tirado JL (1996) *Chem Mater* 8:1429
21. Cullity BD (1978) *Elements of X ray diffraction*. Ed Adison Wesley, USA
22. Pal M, Chakravorty D (2003) *Sādhanā* 28:283
23. Morup S (1994) *Europhys Lett* 28:671
24. Vestal CR, Zhang ZJ (2003) *J Am Chem Soc* 125: 9828